'NCN 941 79-68

Fuel Cluster Design for Improvement of Coolant Void Reactivity and Local Power Peaking

June, 1979

POWER REACTOR AND NUCLEAR FUEL DEVELOPMENT CORPORATION

PNC N941 79-68
Jun., 1979

Fuel Cluster Design for Improvement of Coolant Void Reactivity and Local Power Peaking

Toshio Wakabayashi*
Isao Minatsuki**

Abstract

Single rod substitution experiments have been performed in the Deuterium Critical Assembly in a lattice containing D_2O-moderated and H_2O-cooled 1.5%-enriched UO_2 cluster fuel to investigate the influences of cluster modifications on local power peaking and coolant void reactivity. Both air- and H_2O-cooled 60-pin clusters were substituted at the core center, and measurements were made on critical height changes due to simple removal of their inner fuel pins, insertion of a Gd- or Cd-absorber rod into the central coolant region or replacement of them with an air-filled Al can.

The following are concluded from the present experiment.

(1) The simple removal of the inner fuel pins is effective in reducing local power peaking but not in improving coolant void reactivity.

(2) The insertion of the absorber rod in the central coolant region reduces the coolant void effect without marked increase in local power peaking.

(3) The replacement of the inner fuel pins with the air-filled Al can shifts the coolant void reactivity to the positive side.

The experiment agrees well with the calculation by the code WIMS.

* Heavy Water Critical Experiment Section, O-arai Engineering Center, PNC.

** Present Address: Mitsubishi Heavy Industries Ltd.

I. Introduction

In heavy-water-moderated and light-water-cooled lattices of clustered fuel, local power peaking increases with the number of fuel pins because of increase in neutron flux depression inside the fuel cluster. In addition to the local power peaking, coolant void reactivity is seriously affected by structual alteration of the fuel cluster. A multi-rod fuel cluster with large diameter, which is favorable to increase in channel power, has disadvantage in reducing the void effect and the local power peaking. To apply the multi-rod cluster for an actual reactor effectively, therefore, we need to devise some means to overcome this disadvantage.

Since the local power peaking is essentially related to flux depression due to strong self-shielding of fuel, it can be reduced by diminishing the flux depression inside the fuel cluster. Means applicable to this purpose is the replacement of central fuel pins with scattering material like light-water. Since the central pins produce a relatively small fraction of channel power, we can realize the reduction of the local power peaking by these means without any appreciable loss of the channel power.

As pointed out by Roshd et al[1], the replacement of central fuel pins with scattering material is also effective in reducing void effect of coolant. Adopting these means, we can decrease the two important factors contributing to the positive change in reactivity due to coolant voiding; that is, the increase in fast fission rate and the decrease in resonance absorption rate in uranium 238. In D_2O-moderated and -cooled

CANDU-type lattices, positive change in reactivity is exclusively due to these two factors. Thus, void reactivities in these lattices can be largely improved by the replacement of central fuel pins.

In D_2O-moderated and H_2O-cooled FUGEN-type lattices, however, the improvement of disadvantage factor due to loss of H_2O coolant shifts void reactivity to the positive side besides the two factors. Consequently, we can not sufficiently reduce void effect in the FUGEN-type lattices only by the replacement of central fuel pins. Thus, we need further means to reduce the void effect. Since coolant voiding appreciably decreases flux depression inside the cluster of the FUGEN-type lattice, we expect that decrease in neutron absorption inside the cluster can be diminished by a slender absorber inserted in the center of it and resultantly void effect can be markedly reduced without any noticeable loss of multiplication factor.

To confirm this idea, single rod substitution experiments have been performed in the Deuterium Critical Assembly in a lattice containing D_2O-moderated and H_2O-cooled 1.5 %-enriched UO_2 cluster fuel. Both air- and H_2O-cooled 60-pin clusters were substituted at the core center, and measurements were made on critical height changes due to simple removal of their inner fuel pins, insertion of a Gd- or Cd-absorber rod into the central coolant region or replacement of them with an air-filled Al can. In addition to measurements of critical height changes, local power distribution and thermal-neutron flux distribution were obtained. Experiments are compared with calculations performed by the code WIMS[2].

II. Experimental Procedure

In the present experiments, we prepared the four kinds of test clusters fueled with 1.5 % enriched UO_2. Fig. 1 shows the cross sectional views of these clusters. The schematic drawing of the 54-pin cluster without any central structures is illustrated in Fig. 2. Fig. 3 shows the cross sectional view of the fuel pins assembled into the clusters. As seen in Figs. 4 and 5, the absorber rods inserted in the center of the 54-pin clusters have the same dimensions as the fuel pins. As illustrated in Fig. 4, the Cd-absorber rod consists of aluminum pellets, an aluminum cladding housing them and 0.5 mm-thick Cd rings wrapping the cladding. In the Gd-absorber rod, $Gd_2(SO_4)_3 \cdot 8H_2O$ powder was filled up by means of vibration-packing. The filling-up density of the power is estimated at about 75 percent of theoretical density.

As illustrated in Fig. 6, the test cluster was placed at the center of the Deuterium Critical Assembly and was drived by 136 driver clusters of 28 pins. The driver clusters fueled with 1.2 % enriched UO_2 were housed in air-filled pressure tube, and were arranged in square lattices at a 20.0 cm pitch. Fig. 7 shows the schematic drawing of the Deuterium Critical Assembly with the test cluster being loaded in the assembly. Table I gives dimensions of the core tank, pressure and calandria tubes and fuel pins, and compositions of them.

The reactivities due to coolant expulsion in the test clusters were determined from calibrated changes in D_2O moderator level. That is, reactivity change relevant to

change in D_2O h_1(at 0 % void) to h_2(at 100 % void) were obtained by the formula:

$$\rho(0\% \rightarrow 100\%) = \int_{h_1}^{h_2} (\frac{\partial \rho}{\partial H}) dH = (\frac{\alpha}{2}) [\frac{1}{(h_1+\delta)^2} - \frac{1}{(h_2+\delta)^2}]$$

In this formula, δ is the effective axial extrapolation distances determined by the least-squares method from axial distribution of Cu activity. The axial distribution of Cu activity was measured at the center of the 54-pin cluster without any central structures. Then, α is the constant experimentally determined from reactivity coefficient of D_2O moderator and critical D_2O level. Error in reactivity derived by the above formula is estimated at ±4 %.

Local power distributions inside the 60-pin cluster, and 54-pin clusters with and without Gd-absorber rod were measured by use of enriched uranium-aluminum alloy foils (0.1-mm-thick, 14.8-mm-diam). The enrichment of uranium is 93 % ^{235}U. The foils were packed within fuel pins set at the positions of F-1, F-2 and F-3 for the 54-pin clusters, and F-1, F-2, F-3 and F-4 for the 60-pin cluster. These positions are anti-symmetrically located inside the clusters, as shown in Fig. 1. The foil arrangement within fuel pins is shown in Fig. 9. The uranium foils were wrapped up in aluminum film (0.02-mm-thick) into a cassette, to prevent them from contamination by UO_2 powder and fission products. The cassette of uranium foil was set at the position C in Fig. 9. The Foils were irradiated for 30 min. at 500 W power level ($\sim 10^9$ n/cm^{2}sec). After irradiation, γ-rays from fission products in foils were measured by a 2-in.-diam × 2-in.-thick NaI(Tl) detector.

Thermal-neutron flux distribution was measured inside the test fuel cluster on the surfaces of pressure and calandria tubes, and in D_2O-moderator around them, by use of 0.1 mm-thick dysprosium-aluminum alloy (dysprosium content = 4.0 wt%) Dysprosium-aluminum alloy foils were packed in the same fuel pins and in the same way as uranium foils. In fuel pins, cassettes of dysprosium foils were set at the position B. In addition to bare dysprosium foils as seen in Fig. 9, foils covered with 2.0-mm-wide Cd rings and end-pudding disks were used to measure neutron flux in subcadmium energy region. Thickness of Cd-ring and -disk is 0.5 mm. To measure neutron flux on the surfaces of pressure and calandria tubes, dysprosium foils of 7-mm-diam were set at the two identical positons around each surface, as shown in Fig. 10. Neutron flux in D_2O-moderator region was measured along the 0- and 45 deg. directions, using the same 7-mm-diam foils. In this measurements, foils were arranged with the space of 10 mm in line on 0.5-mm-thick aluminum holder, as shown in Fig. 10. Being suspended from the upper grid plate by fine nylon threads, the holders were accurately and stably positioned between two calandria tubes with two wings protruding from the holder's ends. Fig. 11 illustrates the holders fixed between two calandria tubes. All bare dysprosium foils were irradiated at the same elevation: 60 cm from the lower gird plate. After irradiation, β-rays from ^{165}Dy (half life = 139.9 min.) were counted by a 2-in. -diam × 1/8-in.-thick $CaF_2(Eu)$ scintillator. Measured activities of uranium and dysprosium foils were corrected for background, system dead

time, decay during measuring and efficiency characteristics of various foils like shape and weight. After correction, experimental errors are estimated at ±3 % for local power distribution and at ±2 % for thermal-neutron flux distribution.

III. Results and Discussion

The experimental fractional reduction in void reactivity caused by cluster modifications are compared with a multigroup transport cell calculation, WIMS in Table II. Between the 60-pin cluster and the 54-pin one with the central H_2O-coolant replacing the inner fuel pins, appreciable difference in coolant void reactivity is not observed beyond the experimental error. The replacement of the inner six fuel pins with an air-filled aluminum can makes coolant void reactivity shift to the positive side. On the other hand, the insertion of a Gd- or Cd-absorber rod in the central coolant region replacing the inner six fuel pins makes the coolant void reactivity markedly shift to the negative side. As seen in the Table, the calculations are, as a whole, in good agreement with the experiments.

Measured results of local power distributions and power peaking factors are tabulated in Table III together with the calculations by the code WIMS. The maximum value of local power peaking factor is obtained in the 60-pin cluster without any central structures. The insertion of the Gd-absorber rod slightly increases the local power peaking factor; at most $\sim$4 %. The calculations agree with the experiment within about 4 %.

Fig. 12 shows the dysprosium reaction rate distributions of H_2O- and air-filled 54-pin cluster lattices. These distributions are normalized at the outer surface of the pressure tube.

The only flux distributions in the D_2O-moderator region

which were measured along 0-deg. direction, are shown in Fig. 12, because difference in the flux distribution between 0- and 45-deg. directions is within the experimental error. Thermal-neutron flux depression in the fuel region is larger in the H_2O-filled (0 % void) lattices than in the air-filled (100 %) ones. In the H_2O-filled lattices, furthermore, the thermal-neutron flux seems to be more flattened in the D_2O-moderator region. The tendency of the thermal-neutron flux in the fuel region can be well explained as the diffusion length in the fuel region is shortened by the presence of the H_2O-coolant and resultantly the thermal-neutron self-shielding effect is enhanced[3),4)]. The tendency of the thermal-neutron flux in D_2O moderator region can be regarded as thermal neutrons coming from D_2O moderator are reflected back by H_2O coolant. As further seen in Fig. 12, the thermal-neutron flux depression in H_2O-filled cluster is not much larger at the first layer(F-1) than at the second one. This tendency can be interpreted as the H_2O-coolant in the central region of the 54-pin clusters acts as scattering material rather than neutron absorber.

Fig. 13 shows the dysprosium reaction rate destributions measured in the 54- and 60-pin cluster lattices. In the air-filled lattices, the reaction rates in fuel pins do not differ beyond the experimental error between the 54- and 60-pin clusters. In the H_2O-filled lattices, on the other hand, the reaction rate is clearly larger at the first layer of the 54-pin cluster than at the second layer of the 60-pin cluster although two layers are located at the same distance

from the cluster center. This tendency can be explained as the central H_2O-coolant in the 54-pin cluster makes thermal neutron source larger near the first layer of it, because the H_2O-coolant acts as scattering material. In the D_2O-moderator region, no appreciable difference in the thermal-neutron flux distribution exists between the two lattices.

Fig. 14 shows the influence of the Gd-absorber rod on the dysprosium reaction rate distribution in the 54-pin cluster lattices. In the H_2O-filled lattices, the insertion of the Gd-absorber rod produces no appreciable change in flux distribution in the fuel cluster. In the air-filled lattices, on the other hand, the distribution descends more steeply toward the center in the 54-pin cluster with the absorber rod than without it.

This behavior of the dysprosium reaction rate distributions shows that since neutron absorption by the Gd-absorber rod becomes pronounced due to disappearance of neutron absorption by H_2O-coolant, decrease in neutron flux depression due to coolant voiding confilicts with increase in the neutron absorption by the absorber rod.

This is the reason why the coolant void reactivity is markedly shifted to the negative side by the insertion of the absorber rod in the central coolant replacement the inner fuel pins.

IV. Concluding Remarks

The results of the present experiments are summarized as follows.

1) Simple removal of the inner fuel pins from the 60-pin clusters is not effective in reducing coolant void effect although it appreciably decreases local power peaking in them.

2) To shift the coolant void reactivity to the negative side, an absorber rod needs to be inserted in the central coolant region replacing the inner fuel pins. Increase in local power peaking due to the insertion of the absorber rod is small and permissible.

The present experimental results are useful for the design of new multi-rod fuel clusters which is to be used in the FUGEN-HWR.

Since the calculations by the code WIMS agree well with the experiments, this code is applicable to the nuclear design of the large multi-rod fuel clusters.

Acknowledgement

The authors are much indebted to Dr. K.Shiba and Mr. N.Fukumura for their fruitful discussion. We wish to thank Dr. Y.Hachiya, Mr. Y.Miyawaki and the staff members of the Heavy Water Critical Experiment Section, Oarai, PNC for their support in this series of experiment.

References

(1) M.H.M. ROSHD et al., Trans. Am. Nucl. Soc., 26, 603(1977)

(2) J.R. ASKEW et al., J. BNES, 54, 564 (1966)

(3) T. WAKABAYASHI and Y. HACHIYA, Nucl. Sci. Eng., 63, 292 (1977)

(4) Y. HACHIYA et al., J. Nucl. Sci. Technol., 13, 618 (1976)

Table I Core Dimensions and Compositions

Cluster	
Radius of each layer (60-pin)	
1st	19.2 mm
2nd	38.4 mm
3rd	57.6 mm
4th	76.8 mm
Hanger wire	
Diameter	2.0 mm
Material	Al
Spacer	
Diameter	176.0 mm
Material	Al
Cluster length	2223 mm
Standard fuel meat length	2000 mm
Pressure tube	
o.d.	190.0 mm
i.d.	180.0 mm
Material	Al
Calandria tube	
o.d.	210.0 mm
i.d.	200.0 mm
Material	Al
Moderator	
Material	D_2O
Purity	99.5 mol%
Core tank	
o.d.	3025 mm
i.d.	3005 mm
Height	3500 mm
Material	Al
Upper and lower grid plate	
Material	Al
Temperature	20 °C

Fuel pellet	
Density	10.38 g/cm^3
Diameter	14.77 mm
Enrichment	1.499 wt%
Composition	
^{235}U	1.317 wt%
^{238}U	86.563 wt%
O	12.12 wt%
Fuel pin	
Cladding material	Al
Cladding i.d.	15.03 mm
Cladding o.d.	16.73 mm
Gap material	Air

Table II Comparison of Coolant Void Reactivity between the Fuel Clusters

FUEL TYPE	COOLANT VOID FRACTION (%)	CRITICAL LEVEL (CM)	COOLANT VOID REACTIVITY (0%→100%) (%ΔK/K)	CHANGES IN COOLANT VOID REACTIVITY FROM 60-PIN CLUSTER (%)	
				EXP.	WIMS CALC.
60-PIN CLUSTER	0	136.7	+0.494	—	—
	100	133.9			
54-PIN CLUSTER	0	137.0	+0.485	−1.9	−1.6
	100	134.2			
54-PIN CLUSTER WITH CENTRAL AIR-FILLED Al CAN	0	137.2	+0.519	+5.2	+1.4
	100	134.2			
54-PIN CLUSTER WITH CENTRAL Gd-ABSORBER	0	139.0	+0.432	−12.6	−11.2
	100	136.4			
54-PIN CLUSTER WITH CENTRAL Cd-ABSORBER	0	139.0	+0.381	−22.9	−21.3
	100	136.7			

* $\beta_{EFF}=0.723$

Table III Local Power Distribution

FUEL TYPE	VOID FRACTION(%)	1ST LAYER	2ND LAYER	3RD LAYER	4TH LAYER
60-PIN CLUSTER	0	0.570±0.017	0.656±0.020	0.841±0.025	1.404±0.042 (1.402)
	100	0.636±0.022	0.716±0.025	0.914±0.020	1.297±0.033
54-PIN CLUSTER	0	0.805±0.023	0.785±0.023	1.260±0.025 (1.256)	
	100	0.740±0.022	0.876±0.026	1.223±0.031	
54-PIN CLUSTER WITH CENTRAL Gd-ABSORBER	0	0.715±0.021	0.787±0.024	1.303±0.033 (1.297)	
	100	0.700±0.021	0.862±0.026	1.254±0.032	

( ) : CAL. BY WIMS

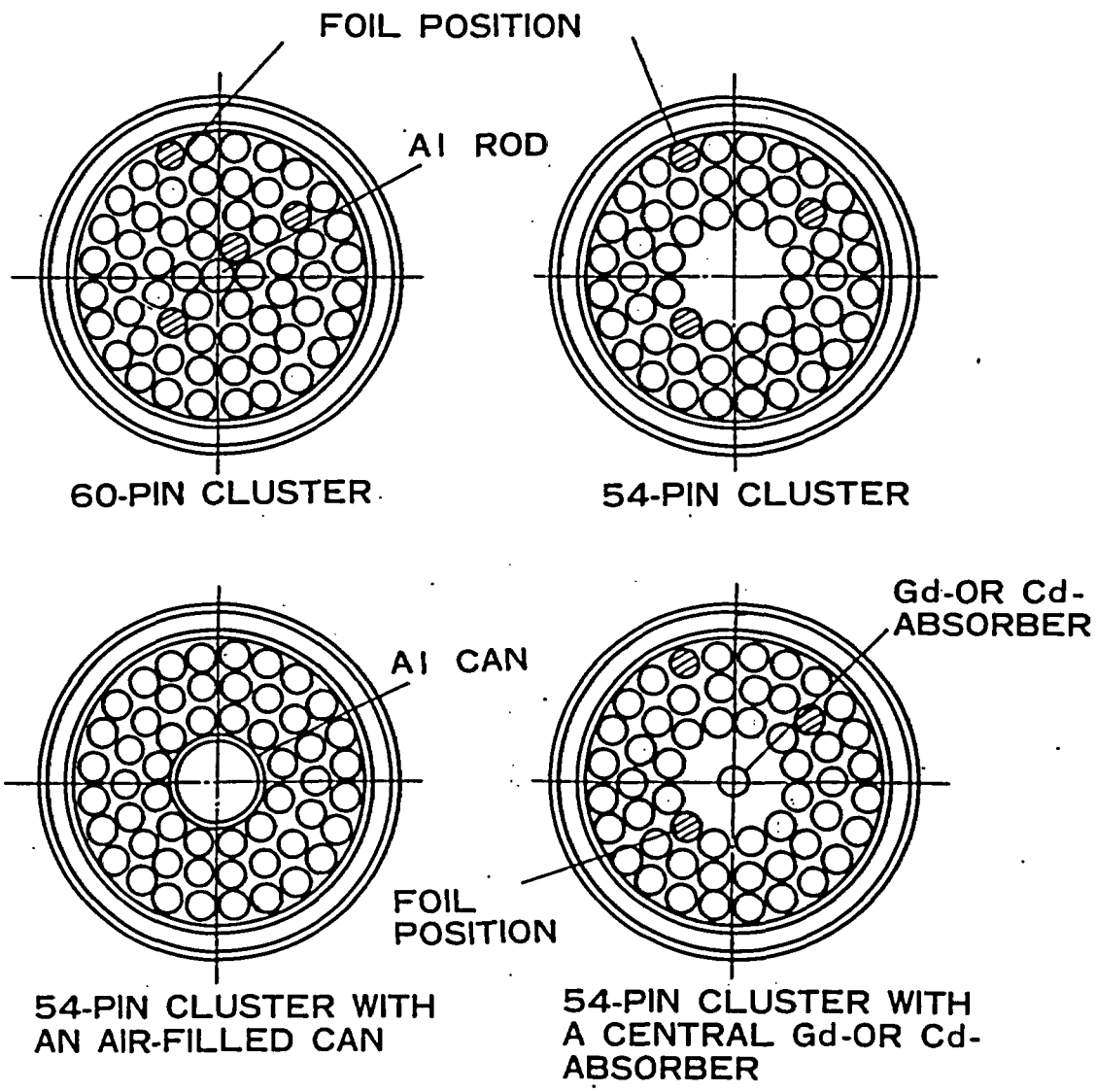

Fig. 1 Cross Section of Test Fuel Clusters

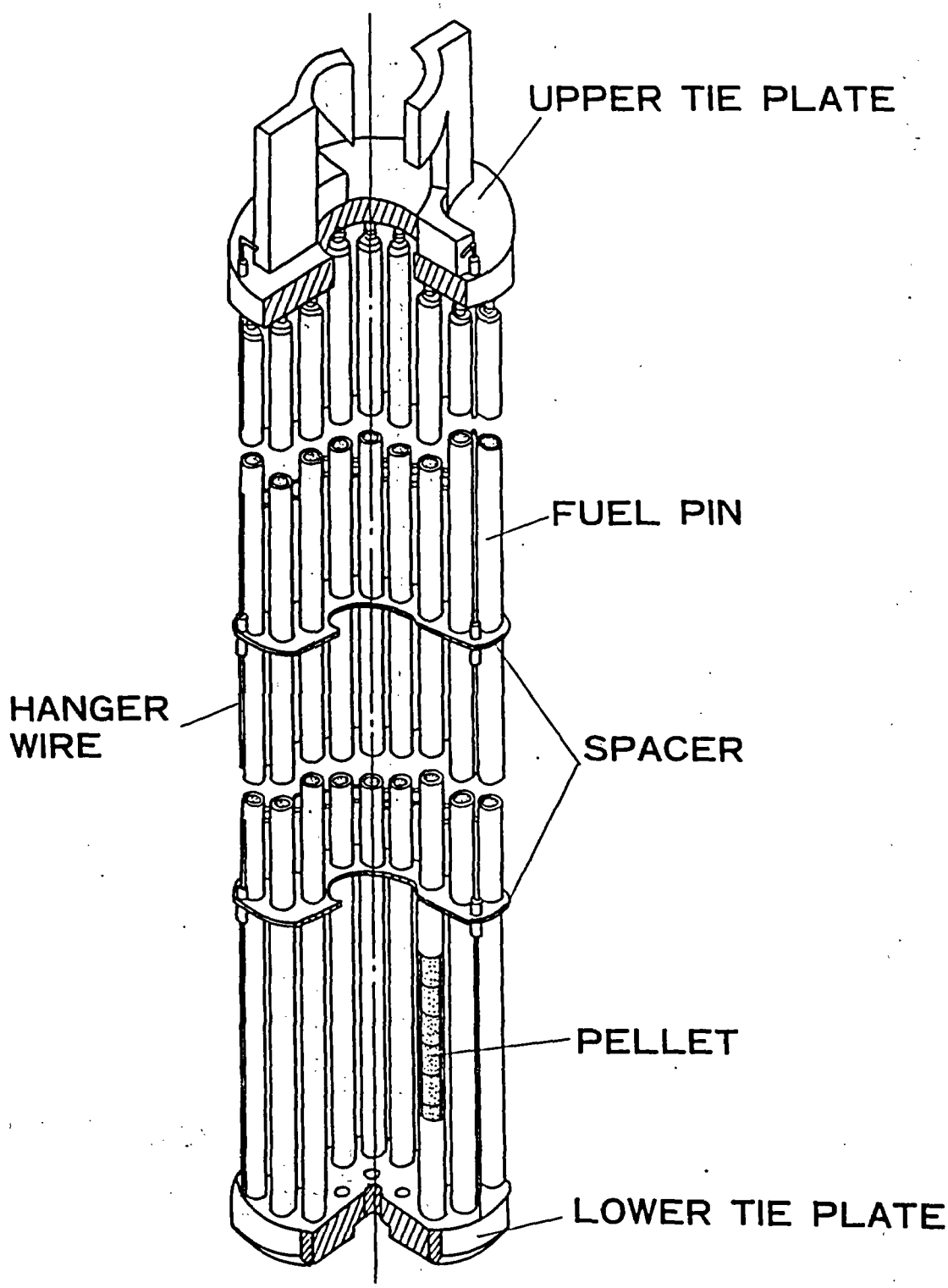

Fig. 2 Schematic Drawing of 54-pin Test Fuel Cluster

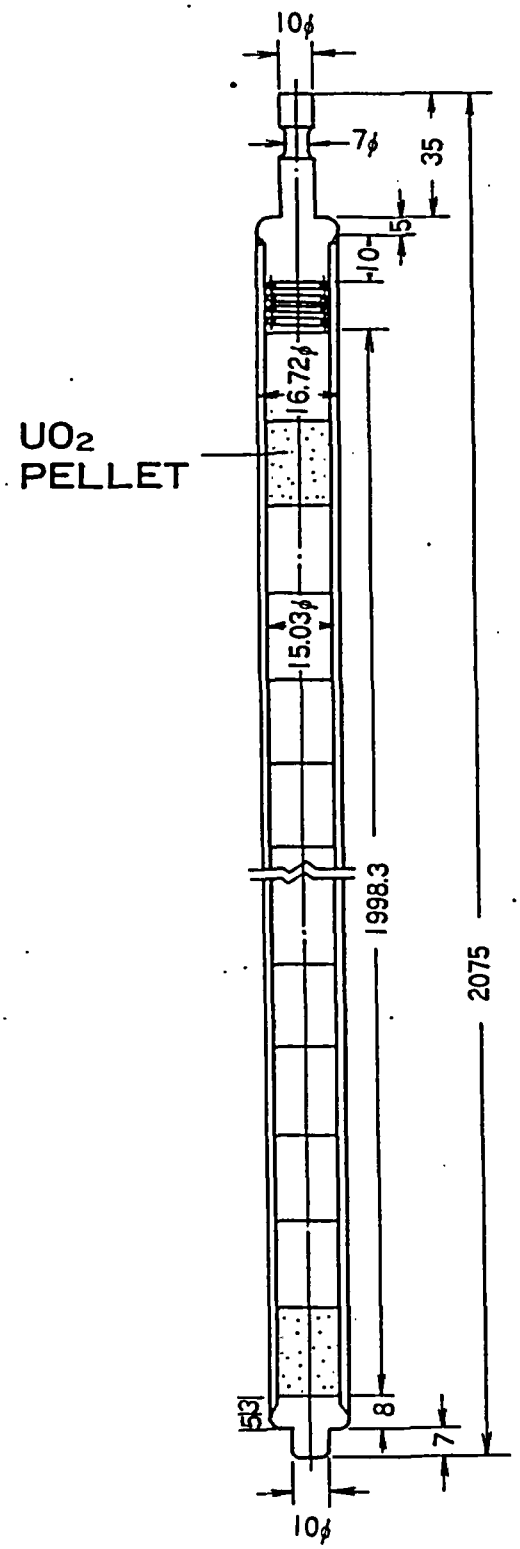

Fig. 3 1.5 wt% UO_2 Fuel Pin

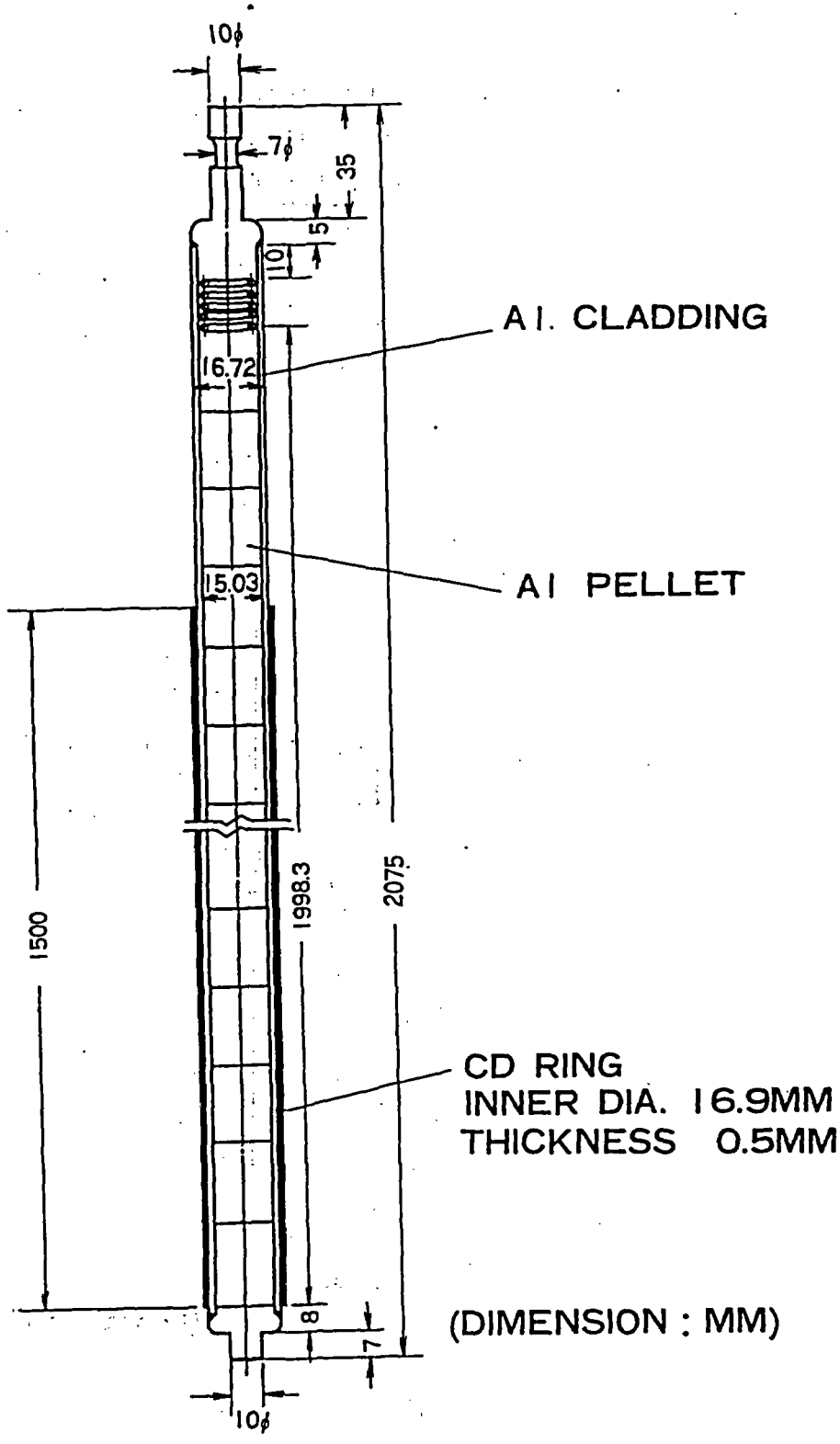

Fig. 4 Cd-absorber Rod

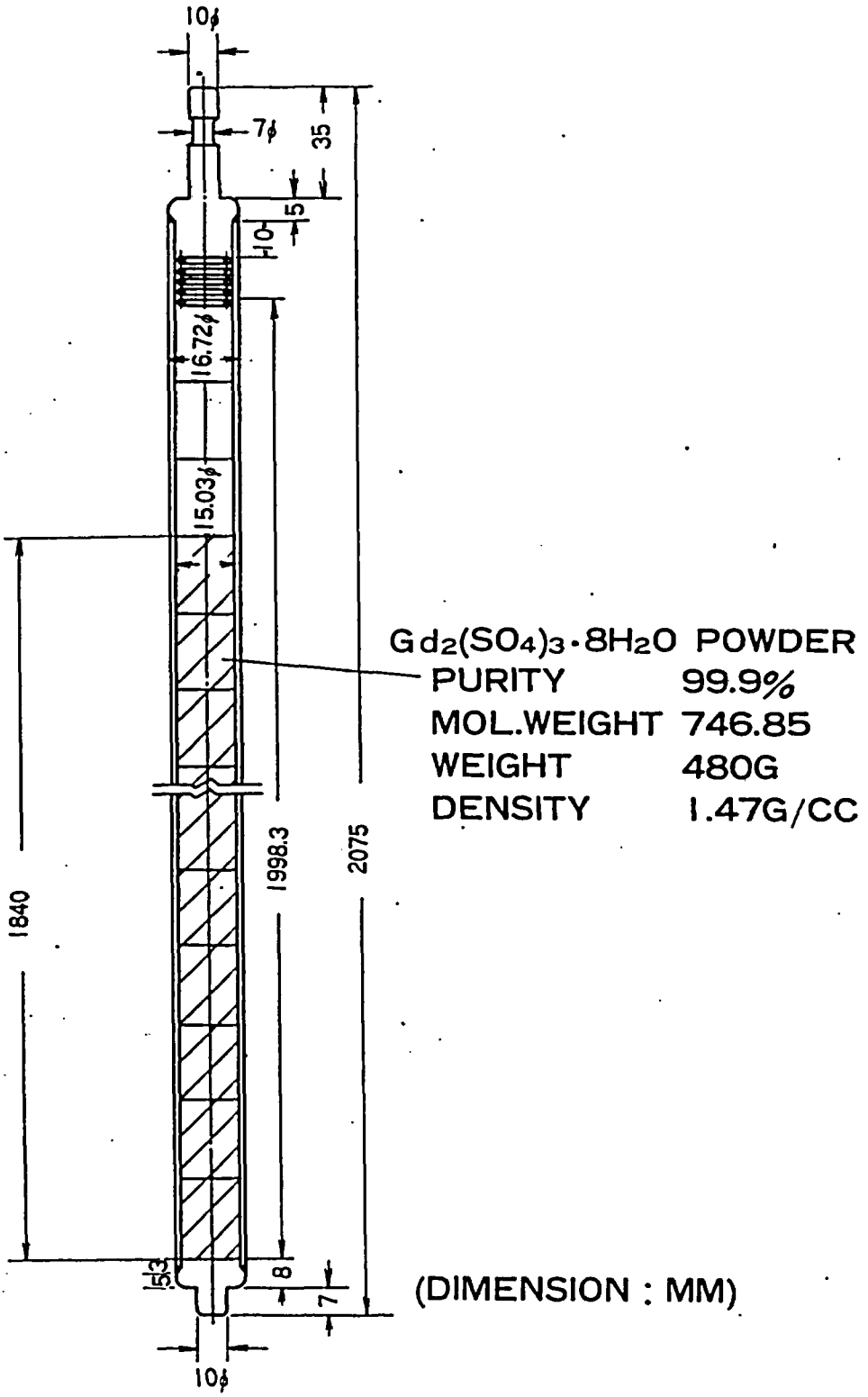

Fig. 5 Gd-absorber Rod

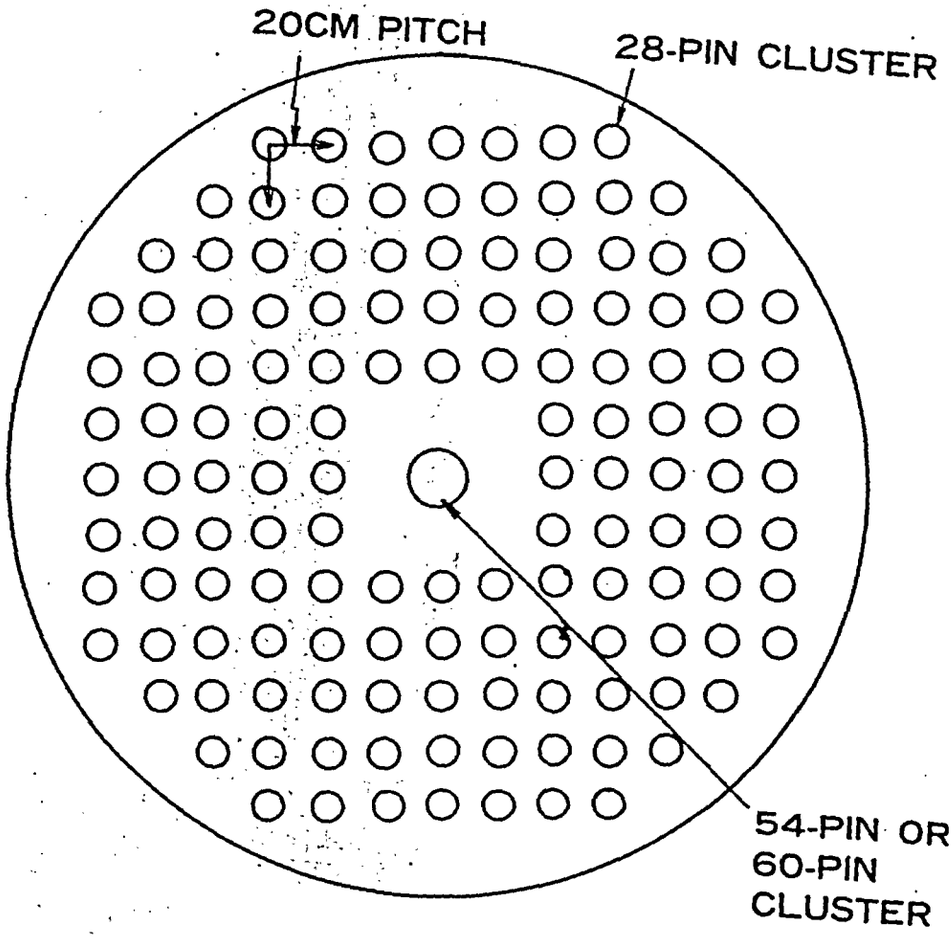

Fig. 6 Core Configuration of DCA

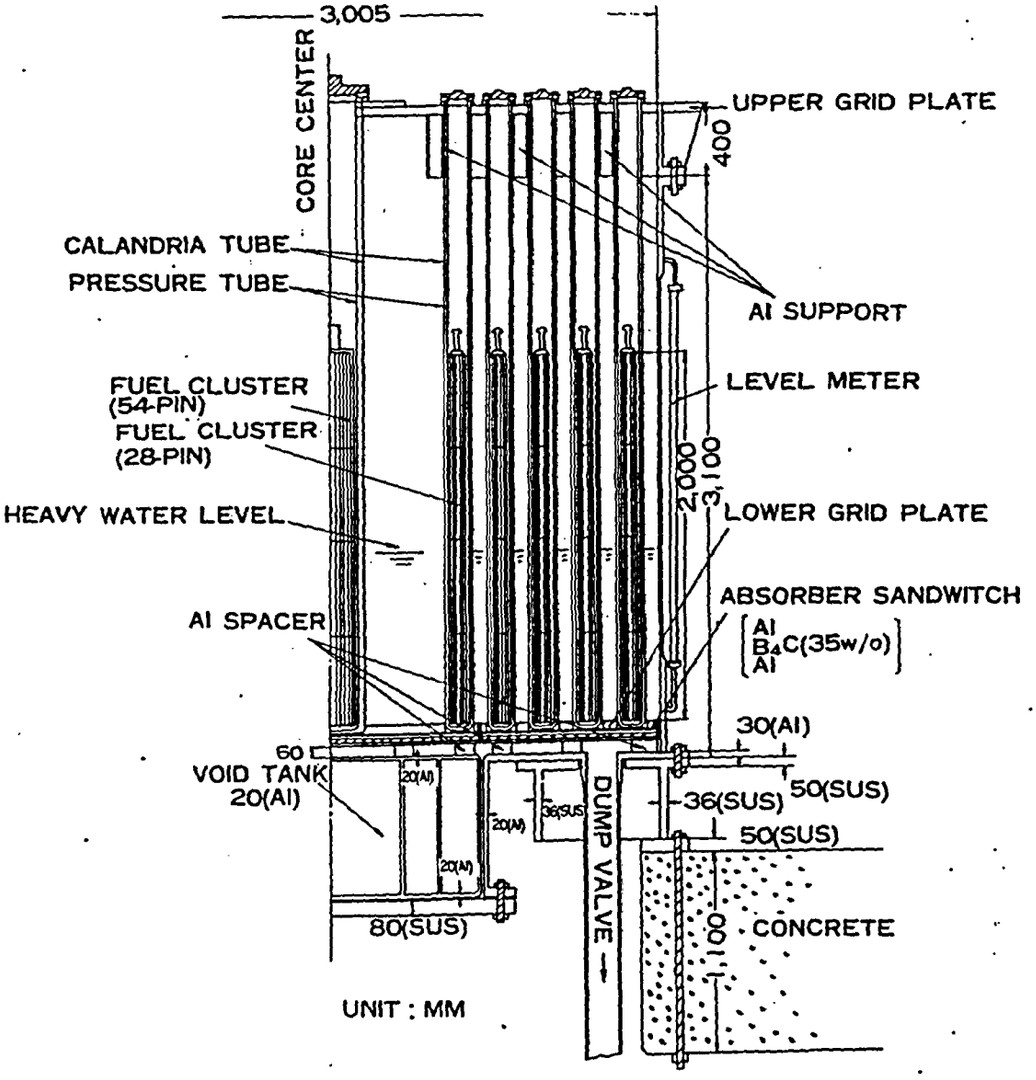

Fig. 7 Schematic Drawing of DCA Core Configuration

Fig. 8 Photograph of Fuel Cluster

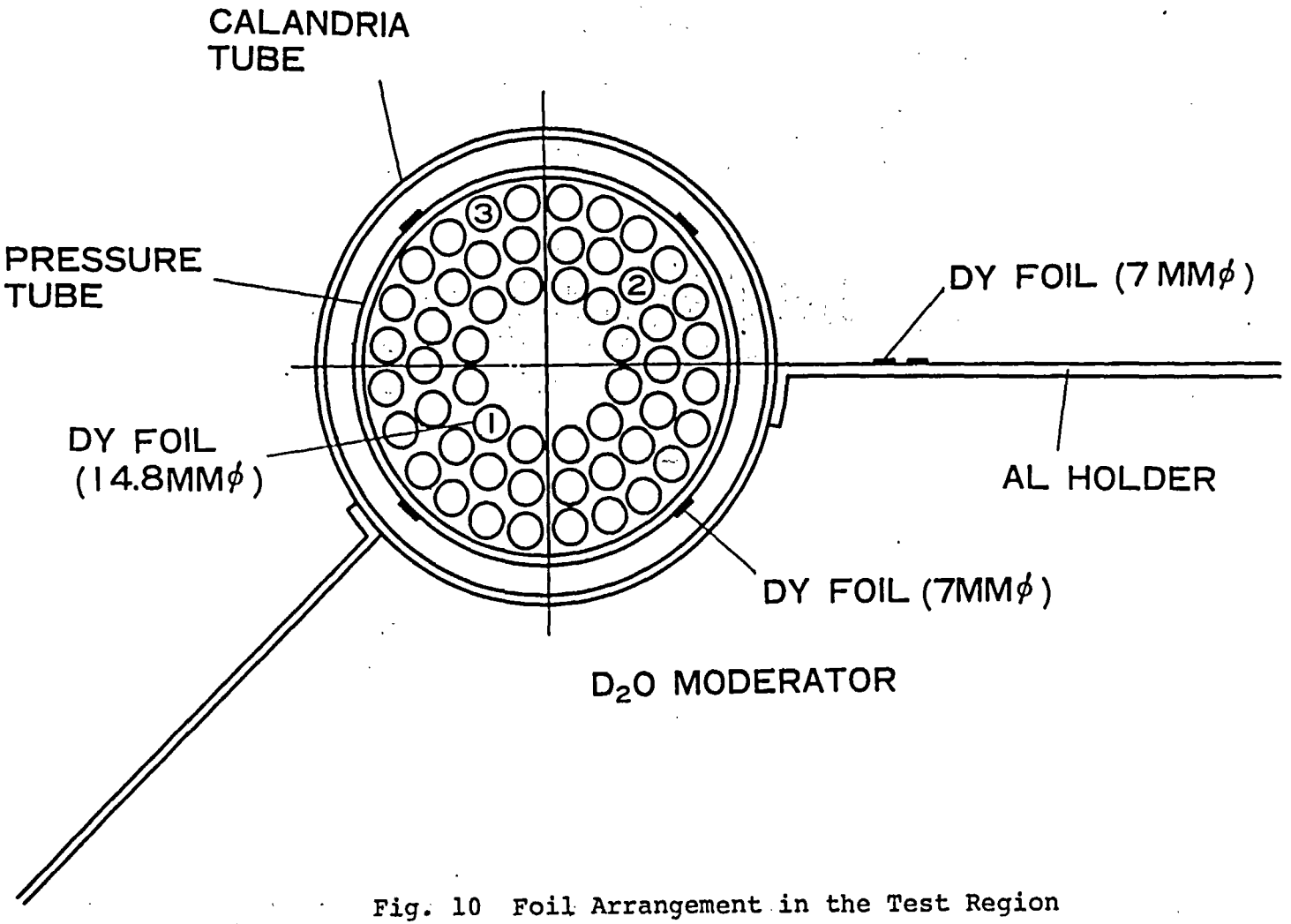

Fig. 10 Foil Arrangement in the Test Region

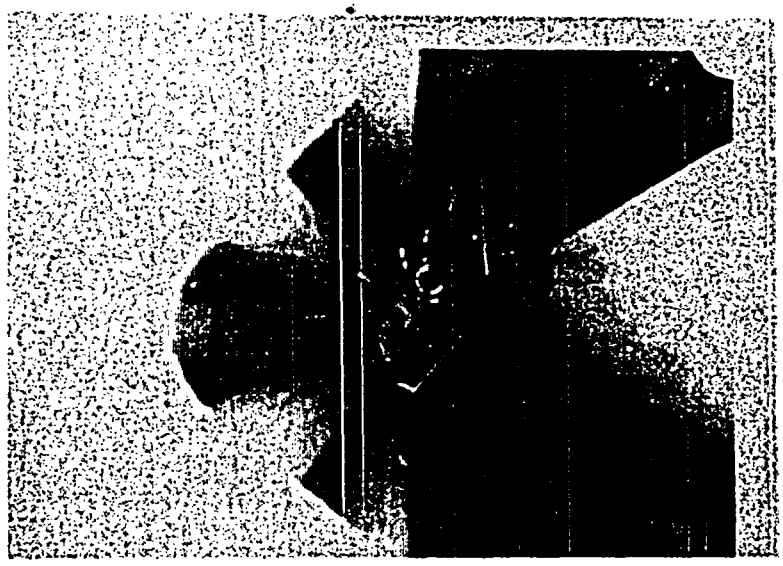

Fig. 11 Arrangement of Al Holder in D_2O Moderator

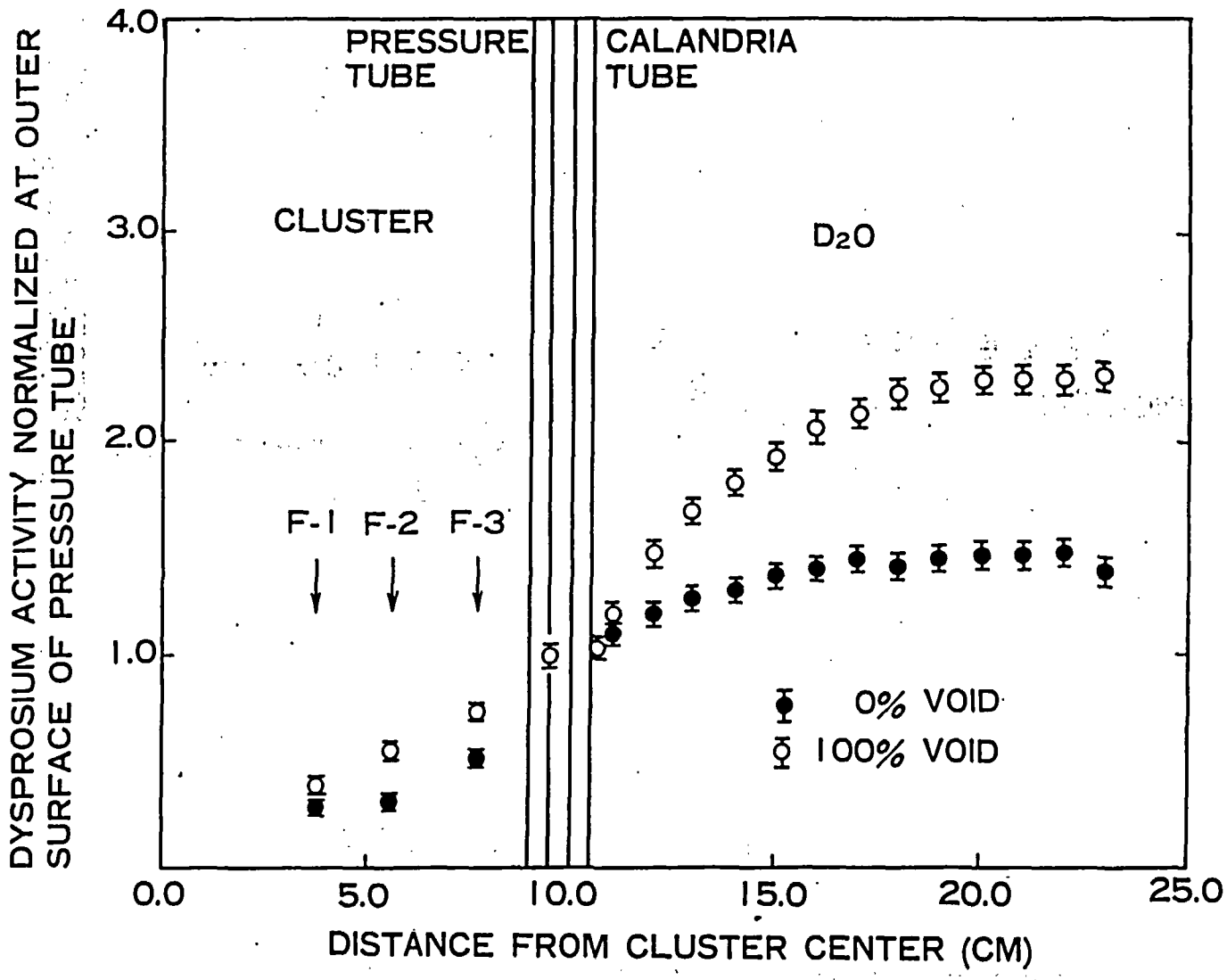

Fig. 12 Dependence of Dysprosium Reaction Rate Distributions on Coolant Void Fraction in 54-pin Cluster

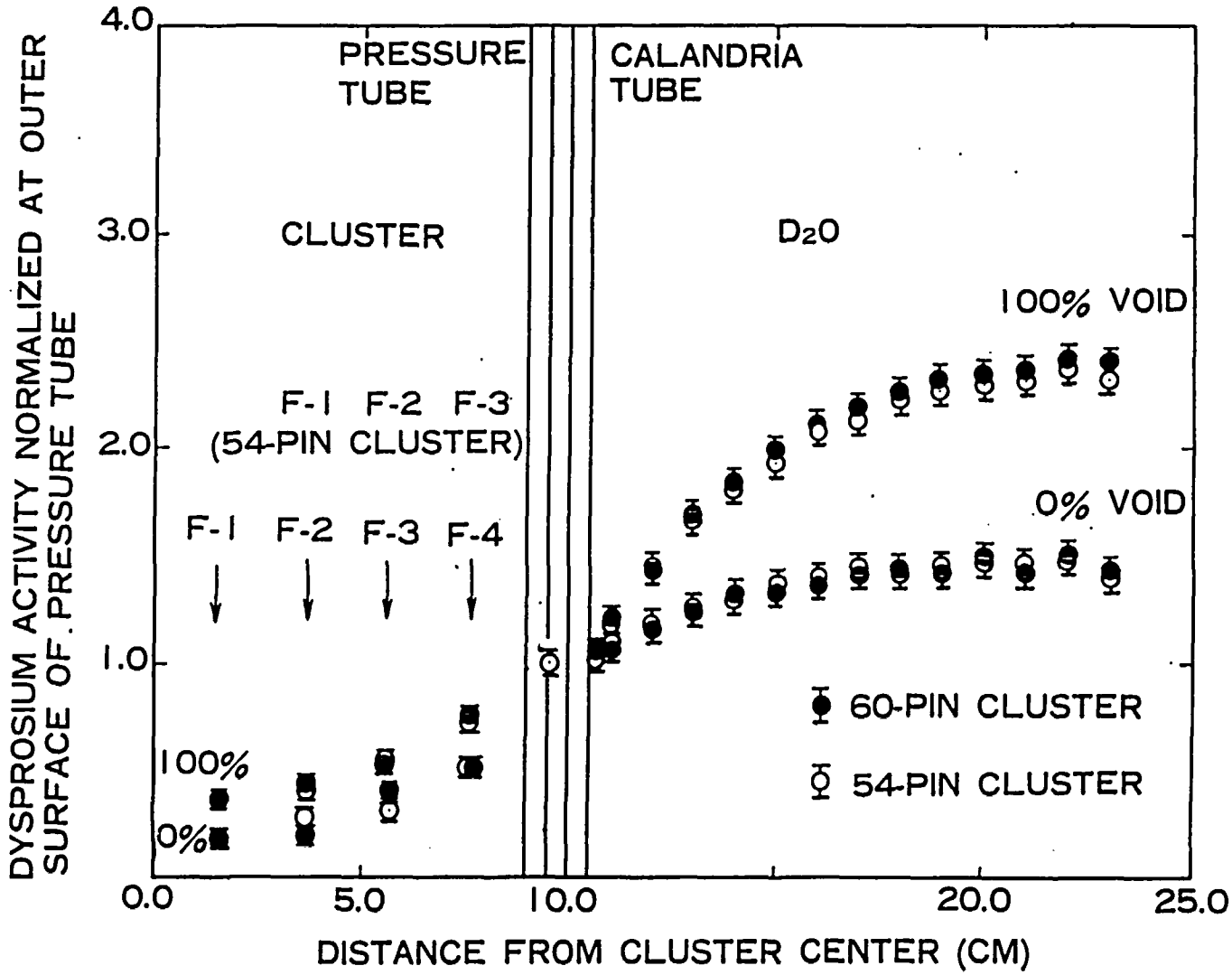

Fig. 13 Dysprosium Reaction Rate Distributions in 60-pin Cluster and 54-pin Cluster

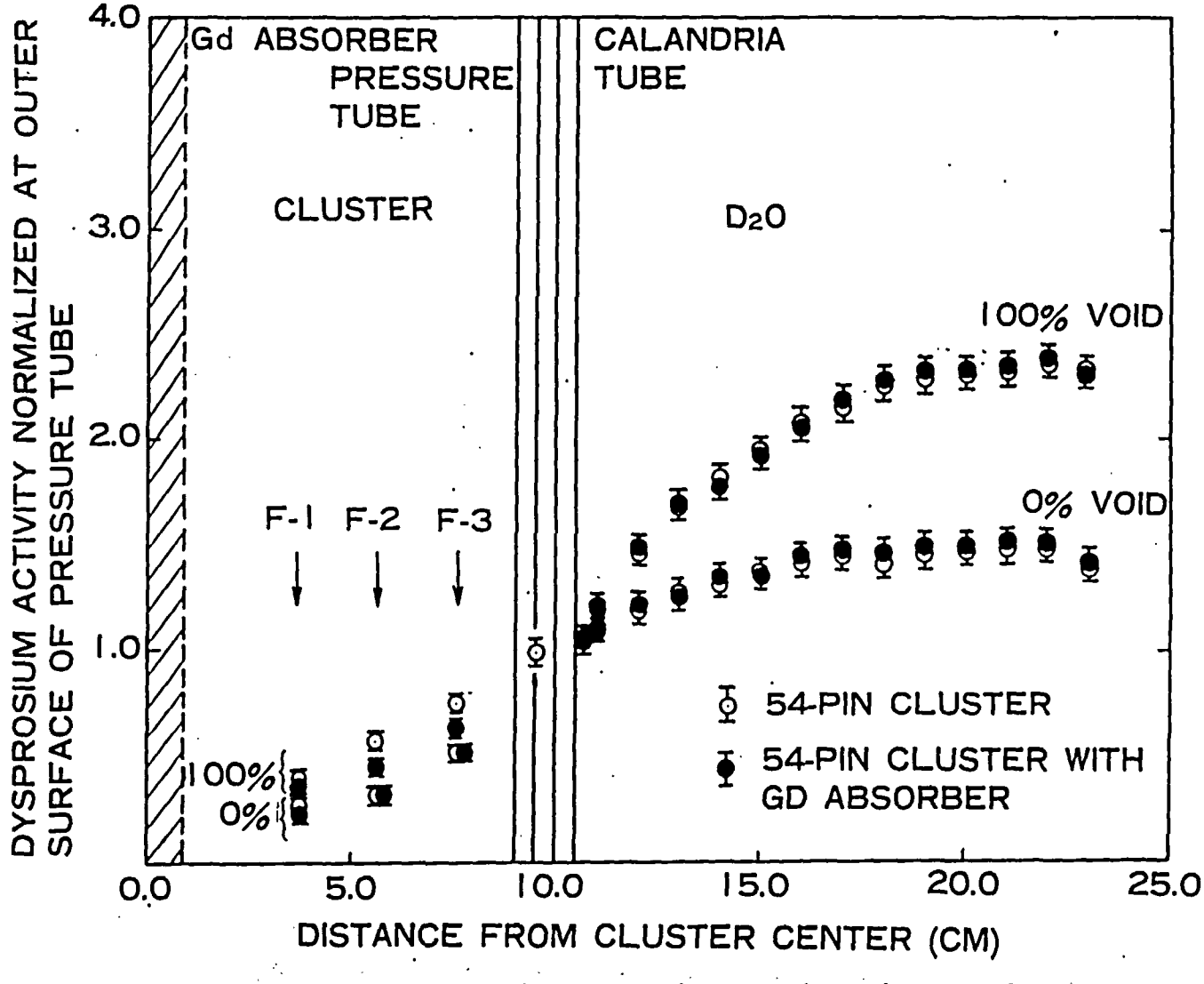

Fig. 14 Dysprosium Reaction Rate Distributions in Normal 54-pin Cluster and 54-Pin Cluster with Gd-Absorber